AD-A248 431

JMENTATION PAGE

Form Approved
OMB No. 0704-0188

on is estimated to average 1 hour per response, including the time for reviewing instructions, searching existing data sources,
eting and reviewing the collection of information. Send comments regarding this burden estimate or any other aspect of this
ucing this burden, to Washington Headquarters Services, Directorate for Information Operations and Reports, 1215 Jefferson
and to the Office of Management and Budget, Paperwork Reduction Project (0704-0188), Washington, DC 20503.

2. REPORT DATE	3. REPORT TYPE AND DATES COVERED
Dec. 15, 1991	Final ; 15 July 1991 - 14 Nov 1991

4. TITLE AND SUBTITLE

Studies of the Polarimetric Dependence of Enhanced
Backscattering from One-Dimensional Surfaces

5. FUNDING NUMBERS

Grant # DAAL03-91-G-0220
Project # G-41-620
R&D Project #1L161102BH57-01

6. AUTHOR(S)

Dr. Kevin A. O'Donnell, Assistant Professor
Dr. Thierry R. Michel, Postdoc

7. PERFORMING ORGANIZATION NAME(S) AND ADDRESS(ES)

The School of Physics
The Georgia Institute of Technology
Atlanta, GA 30332

8. PERFORMING ORGANIZATION REPORT NUMBER

N/S

9. SPONSORING/MONITORING AGENCY NAME(S) AND ADDRESS(ES)

U. S. Army Research Office
P. O. Box 12211
Research Triangle Park, NC 27709-2211

10. SPONSORING/MONITORING AGENCY REPORT NUMBER

11. SUPPLEMENTARY NOTES

The view, opinions and/or findings contained in this report are those of the
author(s) and should not be construed as an official Department of the Army
position, policy, or decision, unless so designated by other documentation.

12a. DISTRIBUTION/AVAILABILITY STATEMENT

Approved for public release; distribution unlimited.

12b. DISTRIBUTION CODE

13. ABSTRACT (Maximum 200 words)

Abstract: We conduct theoretical calculations that study the diffuse scattering properties of surfaces
that are randomly rough in one dimension. The four distinct elements of the Stokes matrix of such
a surface are calculated using numerical techniques that employ exact methods to determine the
scattered field. The behavior of the Stokes matrix elements are interpreted explicitly in terms of
multiple scattering. The surfaces parameters chosen are the same as used in recent experiments.
The investigations clarify the physical origins of disagreement between theoretical and experimental
results in this field.

14. SUBJECT TERMS

Electromagnetic Scattering, Polarization, Rough Surfaces,
Backscattering Enhancement

15. NUMBER OF PAGES

16. PRICE CODE

17. SECURITY CLASSIFICATION OF REPORT	18. SECURITY CLASSIFICATION OF THIS PAGE	19. SECURITY CLASSIFICATION OF ABSTRACT	20. LIMITATION OF ABSTRACT
UNCLASSIFIED	UNCLASSIFIED	UNCLASSIFIED	UL

STUDIES OF THE POLARIMETRIC DEPENDENCE OF ENHANCED BACKSCATTERING

FROM ONE-DIMENSIONAL SURFACES

Final Report

Dr. Kevin A. O'Donnell, Assistant Professor
Dr. Thierry R. Michel, Postdoctoral Researcher

The School of Physics
The Georgia Institute of Technology
Atlanta, GA 30332

92-09266

92   4 10 0 25

THE VIEWS, OPINIONS, AND/OR FINDINGS CONTAINED IN THIS REPORT ARE THOSE OF THE AUTHORS AND SHOULD NOT BE CONSTRUED AS AN OFFICIAL DEPARTMENT OF THE ARMY POSITION, POLICY, OR DECISION, UNLESS SO DESIGNATED BY OTHER DOCUMENTATION.

Accesion For		
NTIS CRA&I	✔	
DTIC TAB	☐	
Unannounced	☐	
Justification		
By		
Distribution /		
Availability Codes		
Dist	Avail and/or Special	
A-1		

TABLE OF CONTENTS

LIST OF FIGURES

1. Introduction and Problem Statement

In work described below, we have investigated the scattering properties of one-dimensional, randomly rough surfaces that produce multiple scattering. It has been shown that a surface with reasonable statistical properties (such as Gaussian statistics and a Gaussian correlation function) may produce backscattering enhancement and related polarization effects. The purpose of this project has been to study the scattering properties of such surfaces using rigorous theoretical methods which take into account multiple scattering and the finite conductivity of the surface. In the calculations to be discussed below, surface parameters are chosen so as to provide a direct comparison with experimental results, thus providing a direct means of determining the current state of agreement or disagreement between theory and experiment.

2. Theoretical Discussion

To second order in the scattered amplitudes, the properties of any scatterer may be completely specified by the matrix relating the incident and the scattered Stokes vectors, which we will refer to as the Stokes matrix of the scatterer. For a planar surface, rough in one dimension, that is illuminated in the plane perpendicular to the grooves of the surface, it is well-known that the Stokes matrix S takes on the simplified form

$$
S = \begin{bmatrix} s_{11} & s_{12} & 0 & 0 \\ s_{12} & s_{11} & 0 & 0 \\ 0 & 0 & s_{33} & s_{34} \\ 0 & 0 & -s_{34} & s_{33} \end{bmatrix} ,
$$

so there are only four unique elements that are of interest. These distinct matrix elements are defined as

$$s_{11} = [<|f_{11}|^2> + <|f_{22}|^2>] / 2 \ ,$$

$$s_{12} = [<|f_{11}|^2> - <|f_{22}|^2>] / 2 \ ,$$

$$s_{33} = \text{Re} [<f_{11} f_{22}^*>] \ ,$$

and $\quad s_{34} = - \text{Im} [<f_{11} f_{22}^*>] \ ,$

where f_{11} and f_{22} are, respectively, the p- and s-polarized scattered amplitudes, and the angle brackets denote an average over the ensemble of surfaces. All matrix elements are implicitly functions of the incident angle θ_0 and of the scattering angle θ_s.

The Stokes matrix elements have been calculated for rough gold surfaces at two different wavelengths ($\lambda = 1.152$ and 3.392 μm). The optical properties of gold at these wavelengths were described by the complex refractive indexes $(n+ik) = 0.312 + i \ 7.93$ and $1.96 + i \ 20.7$, respectively. The statistical properties of the surface profiles were similar to those measured in two recently fabricated surfaces. The stochastic profile had Gaussian statistics and a standard deviation of the surface heights denoted σ; the height correlation function was Gaussian with a transverse correlation length a..

The approach used is based on the numerical calculation of expressions for the scattered field obtained from the exact field equations and from approximate boundary conditions. This Impedance Boundary Condition method has been shown to give reasonable results for the surface statistics and refractive indices considered. The incident beam was of Gaussian form with transverse width $2g$. A realization of the surface profile having the prescribed statistical properties was first evaluated at N_x ($=500$) equally spaced points, the values of the incident and scattered field at the surface were then computed at these points, and the scattered field was obtained as a function of the scattering angle for this realization of the surface profile. This procedure was repeated for N_p ($=4000$) realizations of the surface profile, and the realizations of the scattered field obtained in this fashion were used in the determination of the second moments of the scattered field and of the Stokes matrix elements. The number of points N_x

and the total width of the surface used in the calculations were increased until a sufficient accuracy (1%) was obtained on all four matrix elements; this typically occurred for $\lambda/\Delta x = 10$ (where $\Delta x = L/N_x$) and $L/g = 4$. The ratio of the total scattered power divided by the total incident power was 0.98 and 0.96 for a s and a p-polarized incident beam, respectively.

3. Results

In Fig. 1 we show the matrix elements $s_{11}(\theta_s)$, $s_{12}(\theta_s)$, $s_{33}(\theta_s)$, and $s_{34}(\theta_s)$ calculated in the cases $\theta_0 = 0°$, $10°$, and $30°$, for the surface 711N, and for an incident wavelength of 1.152 μm. Gold's refractive index is $(n + i\kappa) = (.312 + 7.93\ i)$ at this frequency. The ratio of the $1/e$ correlation radius a to the incident wavelength λ is 3.1, and the ratio of the standard deviation of the surface heights σ to a is 0.55. The surface roughness is sufficiently strong to extinguish completely the specular part of the scattered field. The matrix element s_{11} displays a peak in the retroreflection direction $\theta_s = \theta_0$, and this peak as a decreasing magnitude with respect to the background of diffuse intensities when the angle of incidence increases. For small angles of incidence this backscattering peak has two secondary maxima located on either side of the peak, at about 15° from the retroreflection direction. The presence of a backscattering peak and the other features observed in this matrix element have been previously reported in calculations of the s- and p-polarized cross-sections of similar surfaces. Since the matrix element s_{11} is the sum of these cross-sections, the observed behavior may be explained in terms of single and multiple scattering in a similar fashion as in the case of these polarized cross-sections. The element s_{12} is about an order of magnitude smaller than s_{11}, but it is significant and it's angular dependence emerges clearly out of the statistical noise still present after averaging over N_p realizations of the surface profile. This element is the difference between the previously considered s- and p-polarized cross-sections, and its angular dependence includes several sign changes. The matrix element s_{33} has a magnitude which is similar to the magnitude of the other diagonal elements off the Stokes matrix (s_{11}), and it also
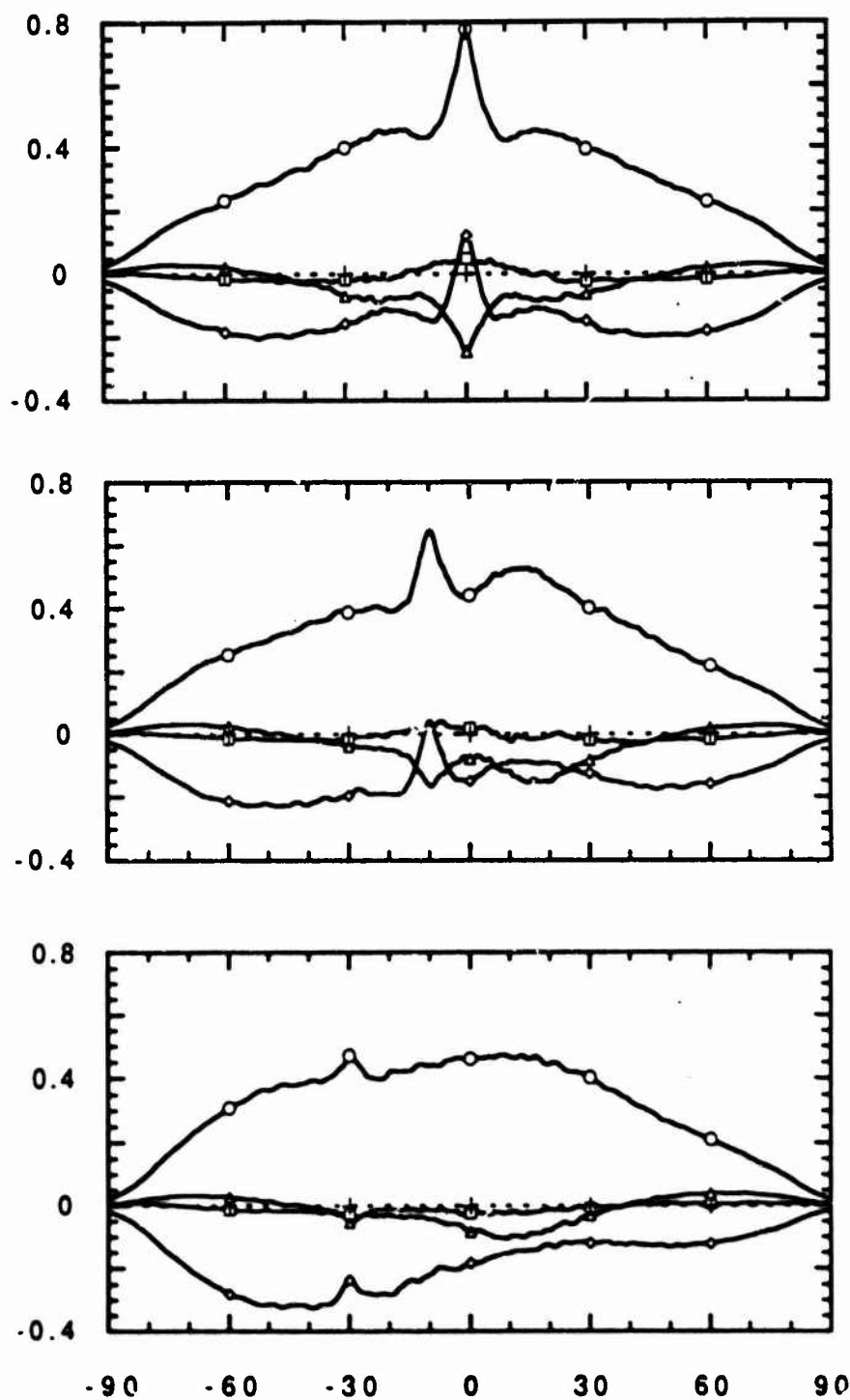
Figure 1. Theoretical calculations of the Stokes matrix elements for a rough surface of roughness $\sigma = 1.95$ μm, $1/e$ correlation radius 3.57 μm, illumination wavelength $\lambda = 1.152$ μm, and gold's refractive index $(n + \iota\kappa) = (.312 + 7.93\,i)$. They are plotted as a function of scattering angle for normal incidence (top), 10° incidence (center), and 30° incidence (bottom). Circles denote s_{11}, squares denote s_{12}, diamonds denote s_{33}, and triangles denote s_{34}. Compare with Figure 2.
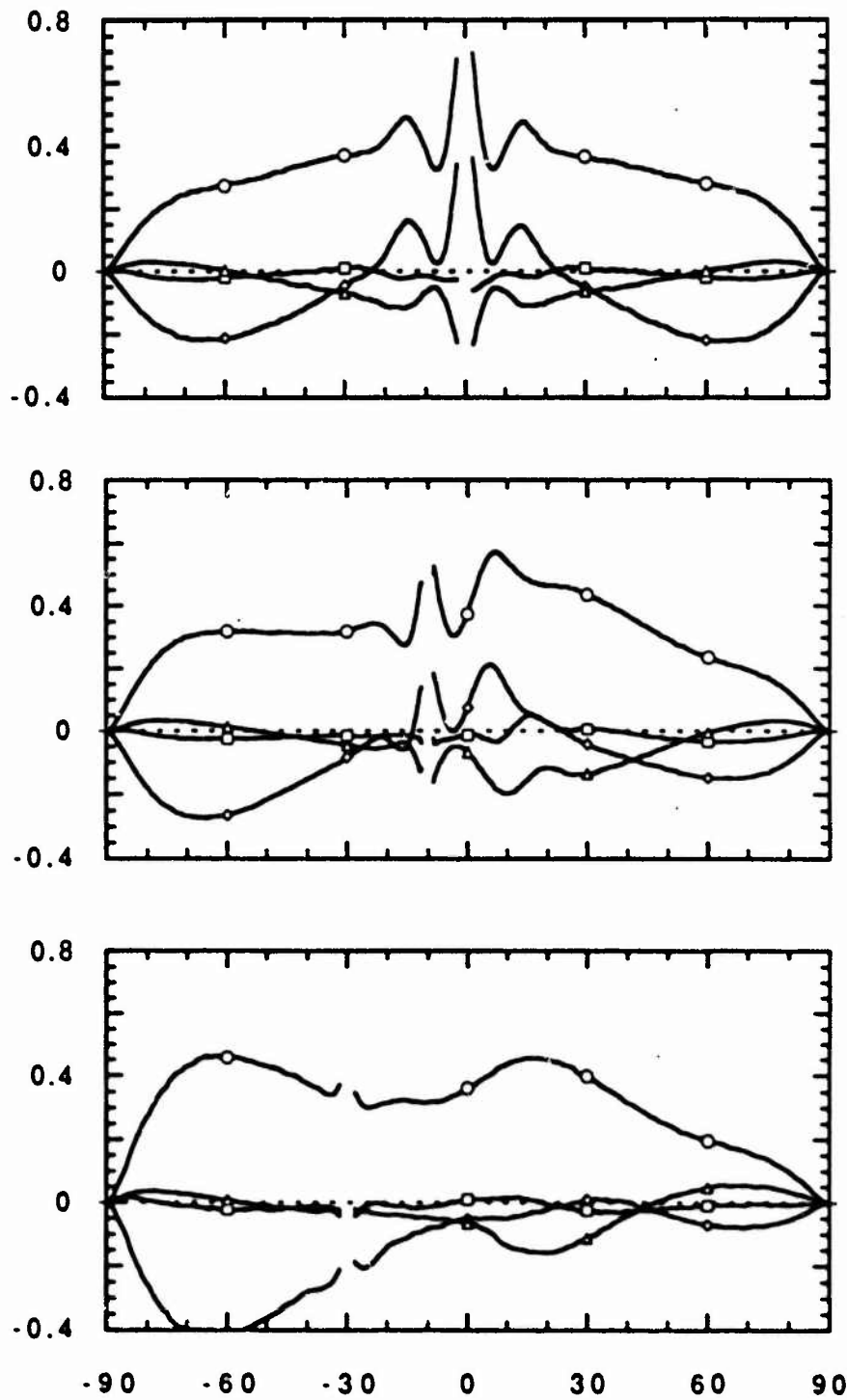
Figure 2. (For Comparison with Figure 1) Experimental results for the Stokes matrix elements for gold surface 711N. Parameters: Roughness $\sigma = 1.95$ µm, $1/e$ correlation radius 3.57 µm, illumination wavelength $\lambda = 1.152$ µm. They are plotted as a function of scattering angle for normal incidence (top), $10°$ incidence (center), and $30°$ incidence (bottom). Circles denote s_{11}, squares denote s_{12}, diamonds denote s_{33}, and triangles denote s_{34}. Normalization assumes unit power of the scattered s-polarized intensity.

displays a very similar structure in the backscattering direction. This matrix element is negative almost everywhere except in the retroreflection direction for small angle of incidence. This behavior may be understood if one consider that gold is highly conducting at this frequency. It was demonstrated in our earlier work that, for a perfectly conducting surface with similar statistical parameters, the main contributions to s_{33} are single and double scattering contributions (with shadowing), as is the case for s_{11}, but that in this matrix elements the single scattering contributions add negatively while the double scattering contributions add positively. The results shown in Fig. 1, demonstrate thus the separability of the single and double scattering contributions in the case of highly conducting surfaces. The effects of the finite conductivity of the surface may be clearly observed in the matrix element s_{34}. Even though the angular dependance of this matrix element are similar when computed for perfectly and finitely conducting surfaces, the magnitude of s_{34} as obtained for the gold surface at this frequency is more than twice that obtained in the perfectly conducting case.

In Fig. 2 the experimental data obtained for the surface 711N, and for an incident wavelength of 1.152 μm, are presented in the cases $\theta_0=0°$, 10°, and 30°; these data may thus be compared to the theoretical results presented in Fig. 1. It is seen that the main discrepancies observed in this cases are the following: the results for s_{11} indicate that the measured scattered intensity is systematically larger at high scattering angle than the calculated one, and related differences occur in the other matrix elements; the enhanced backscattering peak is slightly narrower in the experimental data than in the theoretical results, and the strength of the multiple scattering contributions relative to the single scattering contributions is larger in the experimental data. Some of these discrepancies will be addressed in Figs. 5 and 6.

The theoretical results obtained in the case of the the surface 711N illuminated at a wavelength $\lambda = 3.392$ μm are presented in Fig. 3. As in the case presented in Fig. 1 a backscattering peak located about the retroreflection direction is present in the matrix elements s_{11} and s_{33}. The magnitude of these peaks is seen to decrease when the angle of incidence is increased. The width of the enhancement around $\theta_s = \theta_0$ is significantly larger for the longer
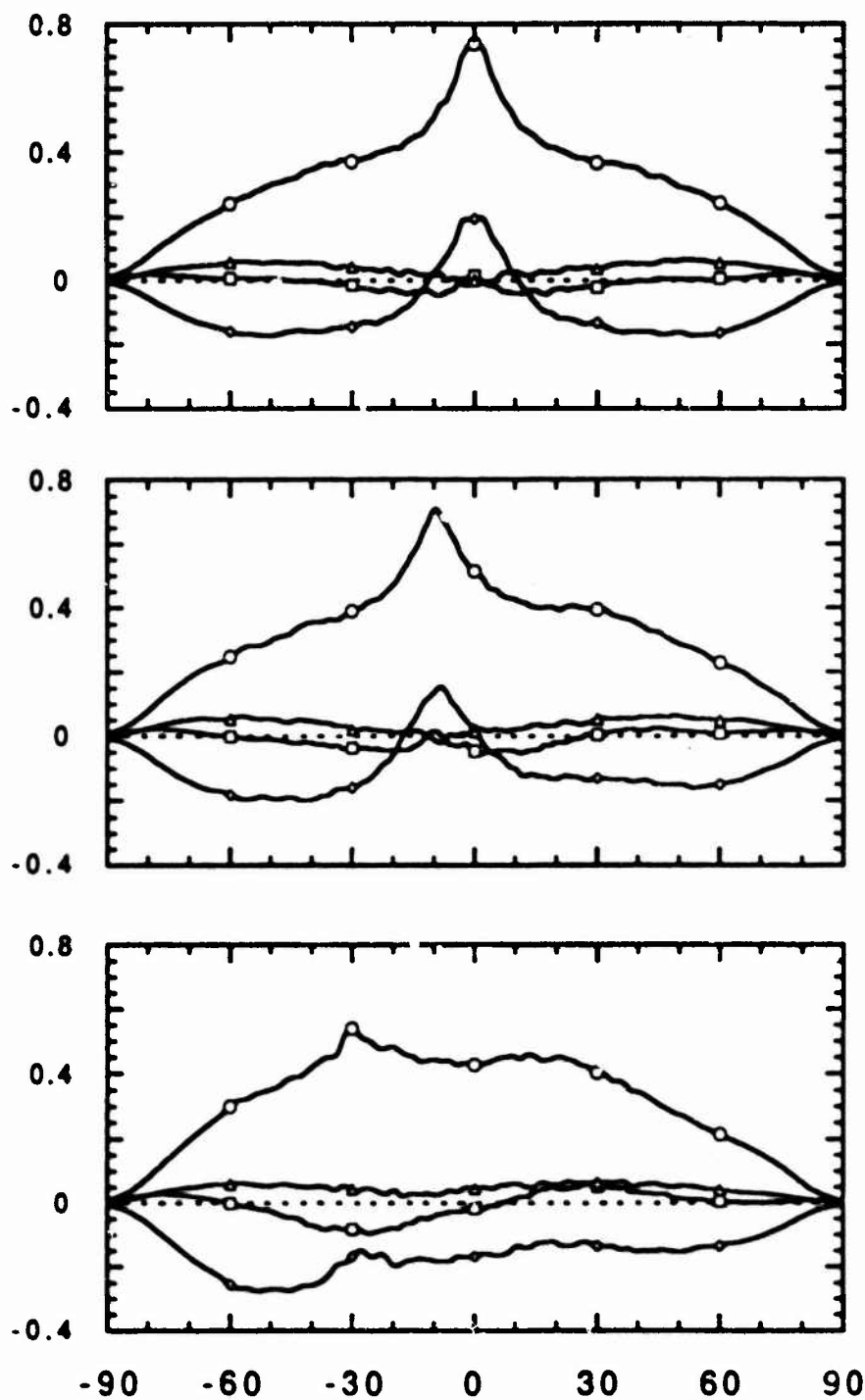
Figure 3. Theoretical calculations of the Stokes matrix elements for a rough surface of roughness $\sigma = 1.95$ μm, 1/e correlation radius 3.57 μm, illumination wavelength $\lambda = 3.392$ μm, and gold's refractive index $(n + i\kappa) = (1.958 + 20.7 i)$. They are plotted as a function of scattering angle for normal incidence (top), 10° incidence (center), and 30° incidence (bottom). Circles denote s_{11}, squares denote s_{12}, diamonds denote s_{33}, and triangles denote s_{34}. Compare with Figure 4.
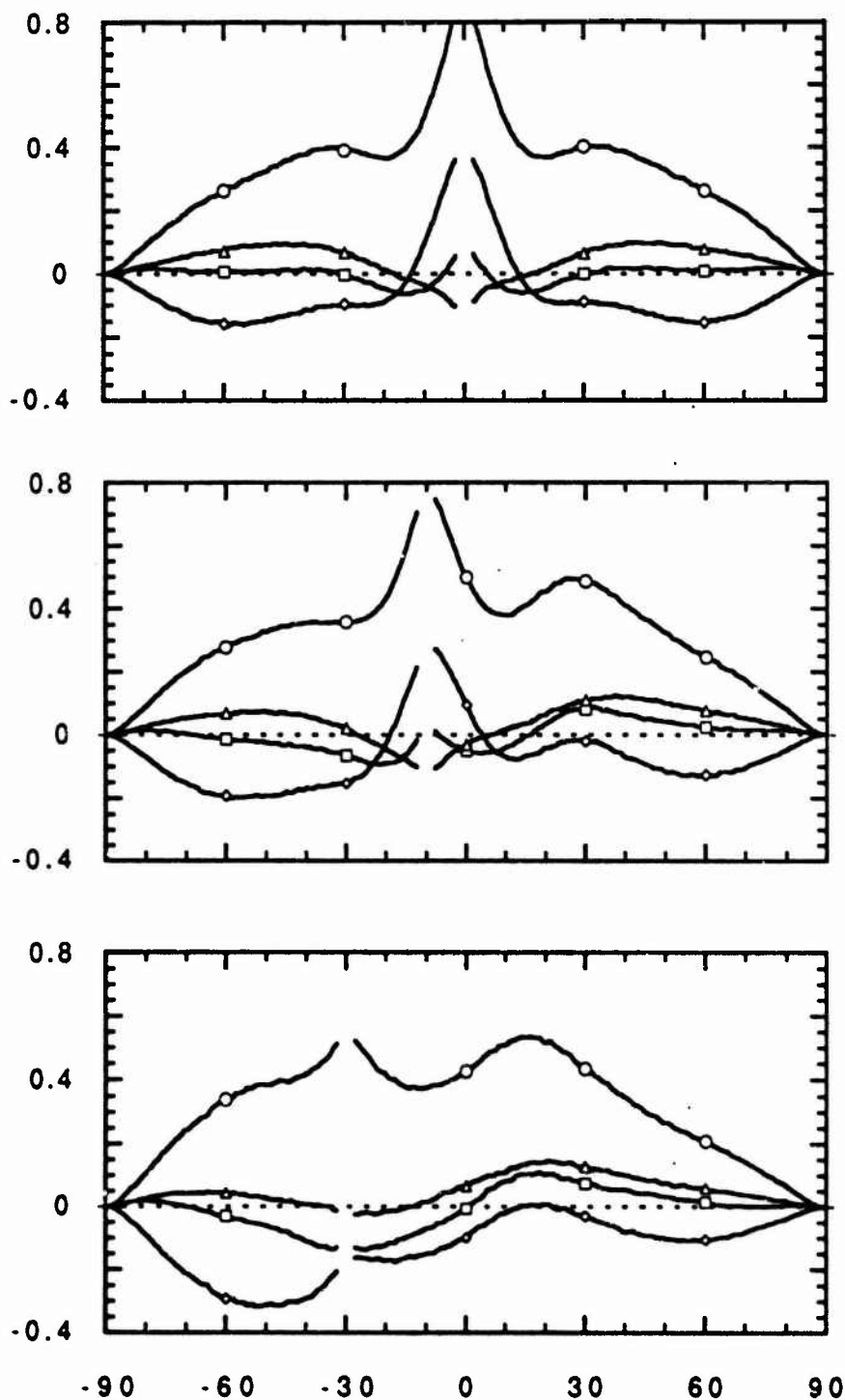
Figure 4. (For Comparison with Figure 3) Experimental results for the Stokes matrix elements for gold surface 711N. Parameters: Roughness $\sigma = 1.95$ μm, $1/e$ correlation radius 3.57 μm, illumination wavelength $\lambda = 3.392$ μm. They are plotted as a function of scattering angle for normal incidence (top), 10° incidence (center), and 30° incidence (bottom). Circles denote s_{11}, squares denote s_{12}, diamonds denote s_{33}, and triangles denote s_{34}. Normalization assumes unit power of the scattered s-polarized intensity.

wavelength; this is consistent with the interpretation of the enhancement as occurring from the double reflection of the light within the grooves of the surface: the typical diffraction width of such a scattering process is λ/a. The off-diagonal elements are a ⁻⁻⁺ an order of magnitude smaller than the diagonal elements but their angular dependence emerges clearly from the statistical fluctuations. Contrary to the case presented in Fig. 1, s_{12} has a narrow backscattering peak (the vertical scale used in Fig. 3 does not allow for the resolution of this peak). The magnitude and the angular dependence of the element s_{34} are different when computed for the finitely conducting surface and for the perfectly conducting surface. Fig. 4 shows the experimental data corresponding to the theoretical results of Fig. 3 for the sake of comparison. The same kind of discrepancies observed when comparing Figs. 1 and 2 are occurring in this case. Th mean scattered intensities measured at high scattering angle are systematically larger than the calculated intensities, and the multiple scattering contributions to the mean intensities are stronger in the experimental data than in the calculations.

Next we present calculations of the matrix elements performed for surface parameters corresponding to surface 226J. This surface is characterized by $a=3.5$ μm and $\sigma=1.7$ μm, and is thus statistically quite similar to surface 711N. These calculations were performed because a slightly different method was used in its fabrication, resulting in a higher quality surface with an actual profile closer to the one-dimensional assumption used in the calculations. It may be seen by comparing the theoretical results for this surface (Fig. 5) to the experimental ones (Fig. 6) that some of the discrepancies have been reduced. In particular the mean intensities measured at high scattering angles for $\lambda = 1.152$ μm are now very close to their calculated counterpart. There are still important differences regarding the strength of the multiple scattering contributions to the mean intensities.

The results presented in Fig. 7 describe the Stokes matrix occurring in the scattering of a beam of light with a wavelength $\lambda = 3.392$ μm. These theoretical results resembles the ones obtained for the surface 711N at this wavelength (Fig. 3), except that there are slightly smaller
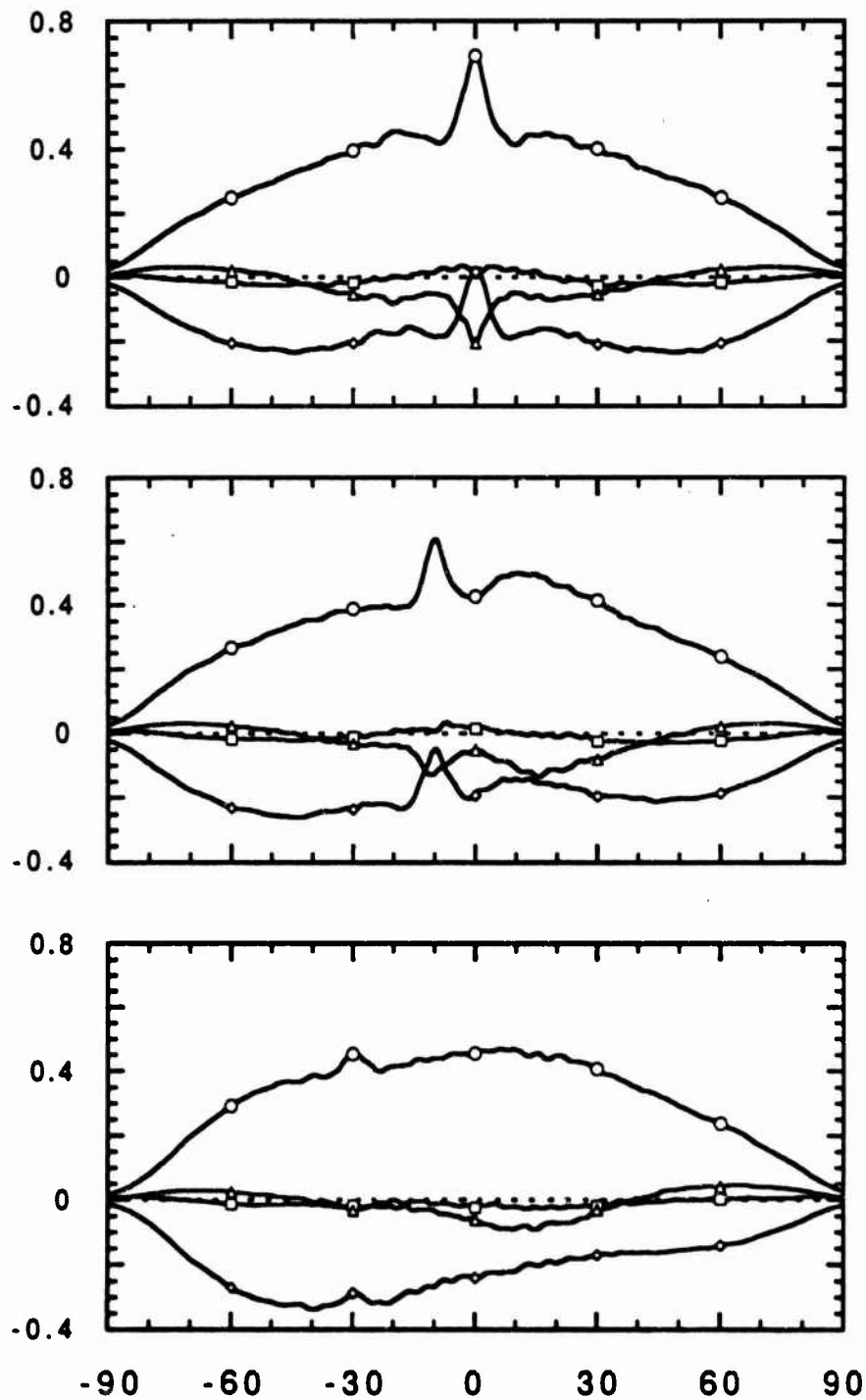
Figure 5. Theoretical calculations of the Stokes matrix elements for a rough surface of roughness $\sigma = 1.7 \, \mu m$, $1/e$ correlation radius $3.5 \, \mu m$, illumination wavelength $\lambda = 1.152 \, \mu m$, and gold's refractive index $(n + i \, \kappa) = (.312 + 7.93 \, i)$. They are plotted as a function of scattering angle for normal incidence (top), $10°$ incidence (center), and $30°$ incidence (bottom). Circles denote s_{11}, squares denote s_{12}, diamonds denote s_{33}, and triangles denote s_{34}. Compare with Figure 6.
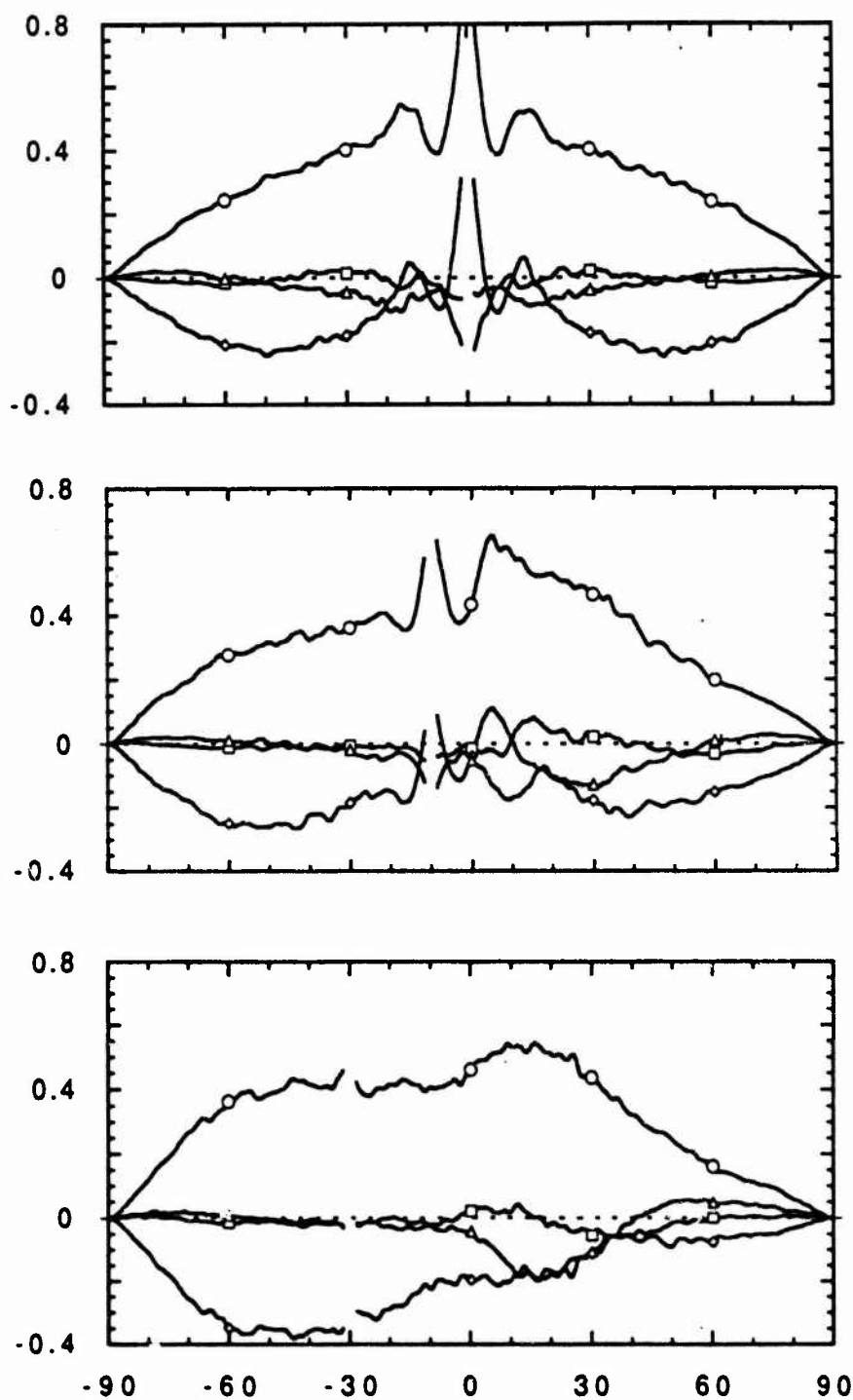
Figure 6. (For Comparison with Figure 5) Experimental results for the Stokes matrix elements for gold surface 226J. Parameters: Roughness $\sigma = 1.7\ \mu m$, $1/e$ correlation radius 3.5 μm, illumination wavelength $\lambda = 1.152\ \mu m$. They are plotted as a function of scattering angle for normal incidence (top), 10° incidence (center), and 30° incidence (bottom). Circles denote s_{11}, squares denote s_{12}, diamonds denote s_{33}, and triangles denote s_{34}. Normalization is from first principles.
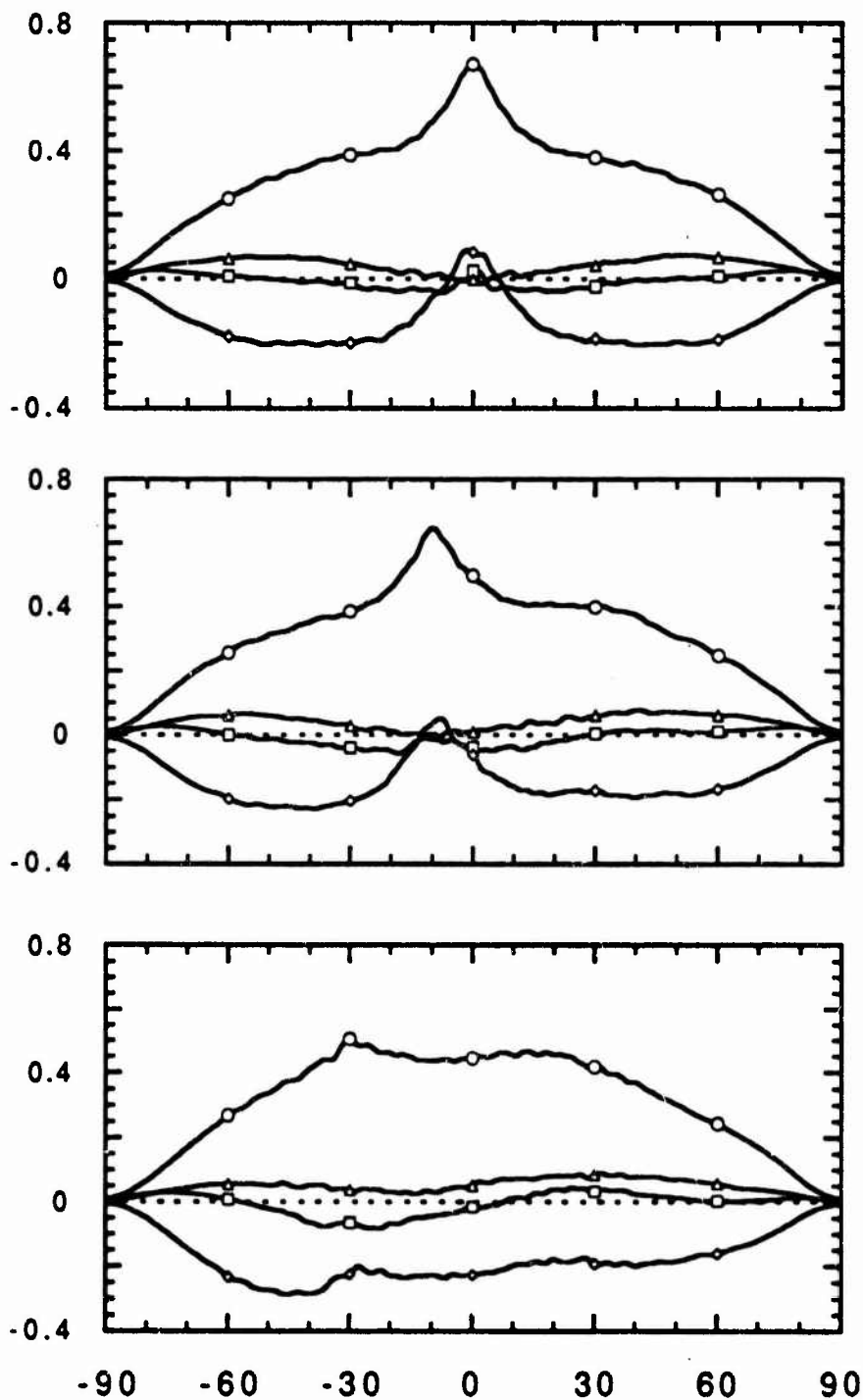
Figure 7. Theoretical calculations of the Stokes matrix elements for a rough surface of roughness $\sigma = 1.7$ μm, $1/e$ correlation radius 3.5 μm, illumination wavelength $\lambda = 3.392$ μm, and gold's refractive index $(n + i\kappa) = (1.958 + 20.7\, i)$. They are plotted as a function of scattering angle for normal incidence (top), $10°$ incidence (center), and $30°$ incidence (bottom). Circles denote s_{11}, squares denote s_{12}, diamonds denote s_{33}, and triangles denote s_{34}.

multiple scattering contributions due to a smaller ratio σ/a. At present time there are no experimental data available for comparison, but experiment will be performed to that effect.

4. Conclusions

In this work we demonstrated that theoretical results may be obtained for the Stokes matrix of a one-dimensional randomly rough surface producing enhanced backscattering when this surface is finitely conducting. The results of these calculations are found to be in good agreement with experimental data, even though some discrepancies regarding the amount of multiple scattering occurring at the surface have been determined. Moreover these results confirm the significance of the Stokes matrix elements of such surfaces. The comparisons of these results with the corresponding calculations obtained in the case of perfectly conducting surfaces allow us to evaluate the role of the finite conductivity of the surface, and to study multiple scattering effects in the scattering of light from highly conducting surfaces. For illumination wavelengths in the infrared, the impedance boundary condition was used for the first time in the kind of simulation calculation that are performed in the study of enhanced backscattering.

5. Publications as a direct result of this work:

T. R. Michel, "The Stokes Matrix Elements of One-Dimensional Rough Surfaces," Poster Paper presented at the ICO Topical Meeting on Atmospheric, Volume and Surface Scattering and Propagation, Florence, Italy, August 27-30, 1991.

M. E. Knotts, T. R. Michel, and K. A. O'Donnell, "The Polarization-Dependence of Light Scattered from Rough Surfaces," International Workshop on Light Propagation and Scattering in Dense Media and Rough Surfaces, Summer School of Laredo, Laredo, Spain, September 2-5, 1991.

T. R. Michel, "Exact Theoretical Calculations of the Stokes Matrix Elements of One-Dimensional, Randomly Rough Surfaces," J. Opt. Soc. Am. A (in preparation for submission in January 1992).

6. Participating Scientific Personnel

Dr. Kevin A. O'Donnell, Assistant Professor (PI)
Dr. Thierry R. Michel, Postdoctoral Researcher

No advanced degrees were awarded during the course of this project.